

Wellesley College Wellesley College Digital Scholarship and Archive

Faculty Research and Scholarship

10-30-2014

First background-free limit from a directional dark matter experiment: results from a fully fiducialised DRIFT detector

James B.R. Battat
jbattat@wellesley.edu

J. Brack

E. Daw

A. Dorofeev

A. C. Ezeribe

See next page for additional authors

Follow this and additional works at: <http://repository.wellesley.edu/scholarship>

Version: Pre-print

Recommended Citation

First background-free limit from a directional dark matter experiment: results from a fully fiducialised DRIFT detector. 30 October 2014.

This Article is brought to you for free and open access by Wellesley College Digital Scholarship and Archive. It has been accepted for inclusion in Faculty Research and Scholarship by an authorized administrator of Wellesley College Digital Scholarship and Archive. For more information, please contact ir@wellesley.edu.

Authors

James B.R. Battat, J. Brack, E. Daw, A. Dorofeev, A. C. Ezeribe, J.-L. Gauvreau, M. Gold, J. L. Harton, J. M. Landers, E. Law, E. R. Lee, D. Loomba, A. Lumnah, J. A.J. Matthews, E. H. Miller, A. Monte, F. Mouton, A. StJ. Murphy, S. M. Paling, N. Phan, M. Robinson, S. W. Sadler, A. Scarff, F. Schuckman, D. P. Snowden-Ifft, N. J.C. Spooner, S. Telfer, Sven Vahsen, D. Walker, D. Warner, and L. Yuriev

First background-free limit from a directional dark matter experiment: results from a fully fiducialised DRIFT detector

J. B. R. Battat^a, J. Brack^b, E. Daw^c, A. Dorofeev^b, A. C. Ezeribe^c,
 J.-L. Gauvreau^d, M. Gold^e, J. L. Harton^b, J.M. Landers^{d,e}, E. Law^d,
 E. R. Lee^e, D. Loomba^e, A. Lunnah^d, J. A. J. Matthews^e, E. H. Miller^e,
 A. Monte^d, F. Mouton^c, A. StJ. Murphy^f, S. M. Paling^g, N. Phan^e,
 M. Robinson^c, S. W. Sadler^{c,*}, A. Scarff^c, F. Schuckman^b, D. P. Snowden-Ifft^d,
 N. J. C. Spooner^c, S. Telfer^c, S. E. Vahsen^h, D. Walker^c, D. Warner^b,
 L. Yuriev^c

^a*Department of Physics, Wellesley College, 106 Central Street, Wellesley, MA 02481, USA*

^b*Department of Physics, Colorado State University, Fort Collins, CO 80523-1875 USA*

^c*Department of Physics and Astronomy, University of Sheffield, S3 7RH, UK*

^d*Department of Physics, Occidental College, Los Angeles, CA 90041, USA*

^e*Department of Physics and Astronomy, University of New Mexico, NM 87131, USA*

^f*School of Physics and Astronomy, University of Edinburgh, EH9 3FD, UK*

^g*STFC Boulby Underground Science Facility, Boulby Mine, Cleveland, TS13 4UZ, UK*

^h*Department of Physics and Astronomy, University of Hawaii, Honolulu, HI 96822, USA*

Abstract

The addition of O₂ to gas mixtures in time projection chambers containing CS₂ has recently been shown to produce multiple negative ions that travel at slightly different velocities. This allows a measurement of the absolute position of ionising events in the z (drift) direction. In this work, we apply the z -fiducialization technique to a directional dark matter search. In particular, we present results from a 46.3 live-day source-free exposure of the DRIFT-II detector run in this completely new mode. With full-volume fiducialization, we have achieved the first background-free operation of a directional detector. The resulting exclusion curve for spin-dependent WIMP-proton interactions reaches 0.9 pb at 100 GeV/ c^2 , a factor of 2 better than our previous work. We describe the automated analysis used here, and argue that detector upgrades, implemented after the acquisition of these data, will bring an additional factor of $\gtrsim 3$ improvement in the near future.

Keywords: dark matter, time projection chamber, DRIFT

*Corresponding author

1. Introduction

There is strong evidence from a variety of sources to suggest that 85% of the Universe’s matter is in the form of as-yet undiscovered dark matter (DM) [1]. One possibility favoured by theories beyond the Standard Model of particle physics is that DM consists of Weakly Interacting Massive Particles (WIMPs) [2]. As such, a large, international effort has been underway for decades to search for the rare, low-energy recoil events produced by WIMP interactions [1]. Several groups have published results in which a handful of events appear above calculated background [3, 4]. Meanwhile, two groups claim to have discovered WIMPs through the use of the annual modulation signature [5, 6]. These latter results are inconsistent with other limits [7, 8, 3].

The goal of directional dark matter detectors is to provide a ‘smoking gun’ signature of DM [9]. Such experiments seek to reconstruct not only the energy, but also the direction of WIMP-induced nuclear recoils, thereby confirming their signals as galactic in origin. Numerous studies have shown the power of a directional signal [10, 11]. Instead of order 10^4 events required for confirmation via the annual modulation signature, only of order 10 – 100 events are required with a directional signature [12]. Additionally, instead of easily mimicked annual modulation, the directional signal is fixed to the galactic coordinate system and is therefore immune to false-positive detections. In recent years, several new ideas for directional detection have been proposed [13, 14]. At present, however, the only demonstrated directional technology is recoil tracking in gaseous time projection chambers [9].

The Directional Recoil Identification From Tracks (DRIFT) collaboration pioneered the use of low-pressure gas TPCs to search for this directional signal [15]. Uniquely, DRIFT utilises negative ion CS_2 drift to transport the ionisation to the readout planes with minimal diffusion [15]. DRIFT has systematically progressed through several epochs of focused R&D: (1) demonstration of stable operation of the first negative ion TPC and, at the m^3 scale, the largest directional detector [15] (2) proof-of-principle of directionality [16, 17] and (3) identification and elimination of detector backgrounds [18, 19, 20, 21]. Presented here are results that constitute a major step forward in stage (3): the first full-volume fiducialiation and background-free operation of a directional dark matter detector.

Background-free operation was made possible by the addition of 1 Torr of O_2 to the nominal 30:10 Torr $\text{CS}_2:\text{CF}_4$ DRIFT gas. This produces several species of so-called ‘minority carriers’ that drift with slightly different velocities relative to the single species observed with the regular gas mixture [22]. An example is shown in Figure 1. With the arrival time difference between the peaks proportional to the distance from the readout plane, these minority carriers enable a measurement of the distance, z , from the readout plane to the ionising event. The z -coordinate measurement enables the removal of all remaining nuclear recoil backgrounds (radioactive decays at the central cathode or in the wire readout planes) from the data, because the backgrounds are localised in z . The detector fiducialisation preserves a large nuclear recoil efficiency, thereby

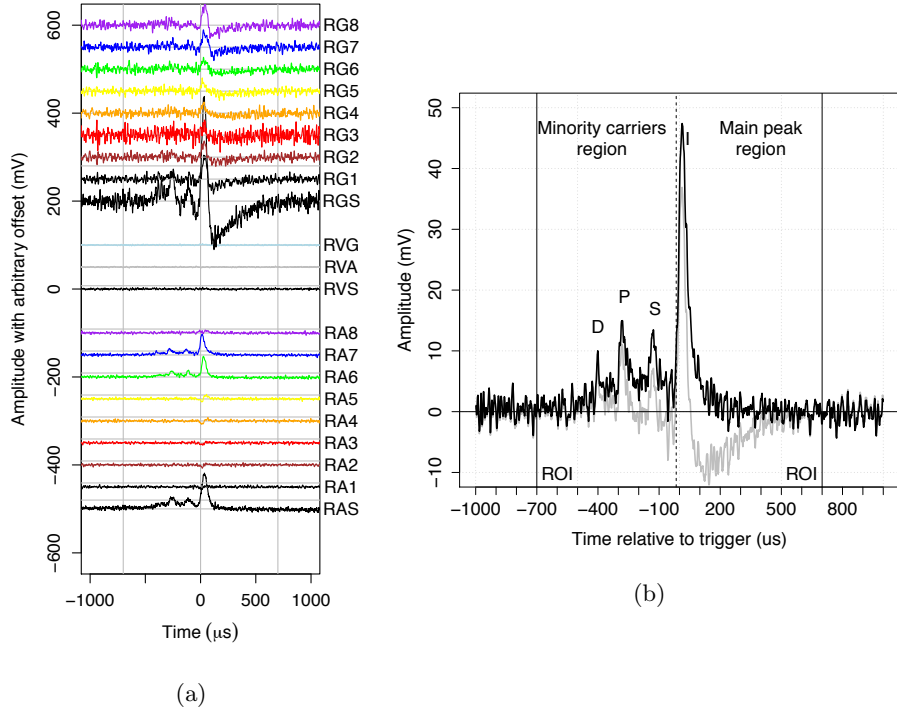


Figure 1: a) Example minority carrier event in the right drift volume, which produced 4980 NIPs at a distance of 35.6 ± 0.2 cm from the right MWPC during a neutron run. In the waveform labels, ‘R’ stands for ‘right’, ‘A’ for ‘anode’, ‘G’ for ‘grid’, ‘V’ for ‘veto’ and ‘S’ for ‘sum’. Horizontal gray lines above the colored anode waveforms indicate the analysis threshold. b) labeled detail of the channel RA7 (blue online) waveform before (grey) and after (black) application of the undershoot removal algorithm discussed in the text. The dotted vertical line separates the minority (S, P, D) peaks from the main (I) peak.

expanding our signal window relative to our previously published limit [23].

2. DRIFT-II detector and science runs

The DRIFT experiment is sited at a depth of 1.1 km in the STFC Boulby Underground Science Facility [24], which provides 2805 m.w.e. shielding against cosmic rays. The TPC is housed inside a stainless steel cubic vacuum vessel, surrounded on all sides with 44 g cm^{-2} of polypropylene pellets to shield against neutrons from the cavern walls. The vessel was filled with a mixture of 30:10:1 Torr $\text{CS}_2:\text{CF}_4:\text{O}_2$ gas, and sealed for the duration of each run. This departure from the normal mode of operation, in which gas is flowed at a constant rate of 168 g d^{-1} , was necessary due to safety concerns over sources of ignition in

the constant flow system. These concerns have since been addressed with modifications to the gas system, allowing us to resume DRIFT-IIId data-taking in continuous-flow mode. The results of these runs will be presented in a forthcoming paper.

The DRIFT-IIId NITPC consists of a thin-film (0.9 μm aluminised Mylar), texturised central cathode [20] at a potential of -31.9 kV faced on either side by two 1 m^2 multi-wire proportional chambers (hereafter, the ‘left’ and ‘right’ MWPCs) at a distance of 50 cm. In this way, two 50 cm drift regions are defined. A field cage of 31 stainless steel rings on either side steps down the voltage smoothly between the central cathode and the MWPCs to ensure a uniform electric field of 580 V cm^{-1} throughout the drift regions. The MWPCs are made up of a central grounded anode plane of 20 μm diameter stainless steel wires with 2 mm pitch, sandwiched between two perpendicular grid planes of 100 μm wires at -2884 V, again with 2 mm pitch and separated by 1 cm from the anode plane. A full description of the detector can be found in Ref. [25].

The inner grid and anode planes have every eighth wire joined together and read out as one, such that a single ‘octave’ of wires reads out $8 \times 2 = 16$ mm in x and y : large enough to contain the recoil events of interest. The outermost 52 (41) wires of the 512 total on the inner grid (anode) planes are grouped together into x (y) veto regions, reducing the fiducial volume of the detector to 0.80 m^3 . The anode and grid veto signals are summed to produce a ‘veto sum’ waveform. All signals are pre-amplified inside the vacuum vessel by Cremat CR-111 preamplifiers, then shaped with a time constant of 4 μs and amplified by Cremat CR-200 Gaussian shaping amplifiers. Finally, the signals pass through a high-pass filter with time constant 110 μs , and are digitised by a 14-bit National Instruments PXI-6133 ADC with input voltage range $-1.25 < V_{\text{in}} < 1.25 \text{ V}$ and sampling rate of 1 MHz, chosen to give good energy and time resolution for signals in the energy range, and of the spatial extent, of interest.

The science dataset consists of 46.3 live-days of sealed, fully shielded operation, with 33.2 g of fluorine in the 0.8 m^3 active volume as a target for spin-dependent (SD) WIMP interactions. The ionisation measurement was calibrated automatically every 6 hours using 5.9 keV X-rays from two shuttered ^{55}Fe sources mounted behind each MWPC. Additionally, 3.2 live-days of neutron calibration data were interspersed with the science runs. During the neutron calibrations, a $\sim 1500 \text{ Bq}$ ^{252}Cf neutron source was placed on top of the vacuum vessel and within the shielding, generating several thousand nuclear recoil events used to determine the WIMP detection efficiency [16]. In addition to providing stability information, these data were used to tune the minority peak analysis.

3. Data analysis

During the 46.3 live-day science dataset, the detector operated in the normal trigger mode in which if any of the voltages on the 16 anode channels (8 in the right MWPC and 8 in the left MWPC) exceeded a fixed threshold of 30 mV, then the signals from all anode, grid and veto channels (3 ms pre-trigger and 10 ms

post-trigger) were written to disk as an ‘event.’ The average rate of events was ~ 1 Hz. Because the total ionisation produced is shared approximately equally between the main and minority peaks, and because the majority of triggered events are near threshold on the main peak, the energy threshold in this run was approximately a factor of 2 larger than in our previously published limit [23], run with the same voltage threshold. An updated triggering scheme has since resolved this issue.

A temporal region of interest (ROI) was defined between -700 μs and $+700$ μs relative to the trigger time. A basic cut was applied to remove events that saturated the ADCs, and the waveforms were subject to noise reduction algorithms that a) remove 55 kHz noise caused by the high voltage power supply, by applying a notch filter to the frequency spectrum, and b) reduce baseline wander by subtracting a sine function from the waveform. These noise reduction techniques allow for an analysis threshold significantly below the 30 mV hardware threshold. The shaping electronics described in Section 2 cause the signals to undershoot the baseline, mainly due to AC coupling. This undershoot was corrected prior to event reconstruction using a two-stage undershoot removal algorithm implemented in software. The algorithm uses time constants measured on a channel-by-channel basis. Figure 1b shows that this filter successfully restores the baseline. Further basic cuts were applied to remove events that a) crossed a 15 mV veto sum threshold (x and y fiducialisation), b) extended outside the ROI, c) had hits on both sides of the detector, d) had non-contiguous channel hits, e) had hits on all 8 anode channels, and f) had risetime < 3 μs , consistent with an impulse charge deposition. These basic cuts are referred to collectively as ‘Stage 1’ cuts, and are designed to have very high acceptance for nuclear recoils.

To reconstruct the number of ion pairs (NIPs) in an event, we select the anode channels that cross the analysis threshold of 9 mV, and integrate the anode waveform across the ROI. The final NIPs value for the event is the sum of these integrated values, scaled by a calibration constant. This constant was calculated every 6 hours using the 5.9 keV X-rays from the ^{55}Fe calibration sources [18] and a W-value of 25.2 eV. The W-value is the average energy required to produce an electron-ion pair in the gas. The W-value for a 30:10 Torr $\text{CS}_2:\text{CF}_4$ mixture was used for this calculation [26] because no measurement has yet been made for 30:10:1 Torr $\text{CS}_2:\text{CF}_4:\text{O}_2$. This will be addressed in a forthcoming paper. However, the results of Refs. [27, 28, 29] suggest that the addition of 1 Torr O_2 will change the W-value by $\sim 1\%$, which is a factor of two smaller than the uncertainty of the W-value used here [26]. Fluctuations in the ^{55}Fe energy measurement were observed at the $\sim 4\%$ level over the course of the full 46.3 live-day dataset, which demonstrates the stability of the calibration. Table 1 shows how the NIPs yield varies with energy of the recoiling particle. It is based on calculations in Ref. [30], as validated experimentally in [23].

The use of z fiducialisation has increased the signal acceptance relative to Ref. [23] by replacing a set of low-efficiency cuts that had been necessary to remove background events from the electrodes, with a reduced set of straightforward, high-efficiency cuts described below. The ratio between the ionisation

Fluorine recoil energy (keV _r)	NIPs
10	140
20	332
50	1055
100	2528
150	4165
200	5852

Table 1: NIPs yield as a function of energy for fluorine recoils, from Ref. [30].

measured in the minority peaks to that measured in the I peak on the channel with the highest maximum voltage in the ROI (see Figure 1) was found to be a powerful parameter for discriminating between nuclear recoils caused by calibration neutrons and background events such as sparks [22]. Events for which this ratio was < 0.4 were cut. One further high-efficiency cut was added to ensure that the ionisation detected on the grid was in agreement with that detected on the anode, which removed a residual population of oscillatory background events described in Ref. [31].

An event passing the preceding set of cuts had its maximum amplitude channel’s waveform passed to a peak-fitting algorithm, which used a three-Gaussian fit to find the arrival times of the I, S and P peaks at the anode. The D peak was not used, since its amplitude was often within the noise. The time difference between any two peaks can be used to calculate the event’s z position using:

$$z = (t_a - t_b) \frac{v_a v_b}{(v_b - v_a)}. \quad (1)$$

Here, a and b represent two different carrier peaks (I, S or P), and t and v are the arrival time relative to trigger, and drift velocity, respectively. In practise, the I and P peaks were used, since the S peak is suppressed for events with high z [22]. Events for which the algorithm failed to calculate a z position were cut, which removed all science-run events other than the well-understood radon progeny recoils (RPRs) and low-energy alphas (LEAs) [18] from the background dataset, whilst preserving an estimated $\sim 70\%$ of recoil-like events from the neutron calibration runs. The algorithm removes events in which it does not find 3 equidistant peaks (I, S, P), which results in a reduction in efficiency at high- z . However, the main source of failed z reconstruction was events occurring near the MWPCs, since their charge peaks overlap temporally, and cannot be distinguished in this analysis.

The z measurement was calibrated in-situ during the science runs using a selected sample of RPR/LEA events that are known to be centred on the central cathode at $z = 50$ cm. The observed RMS of the z -coordinate of the RPR/LEA events was 1 cm, consistent with the size of ripples on the thin-film central cathode. Based upon the uncertainty on the I and P peak means in the three-Gaussian fit, the precision in the measurement of z is 1.6 mm. The z vs. NIPs

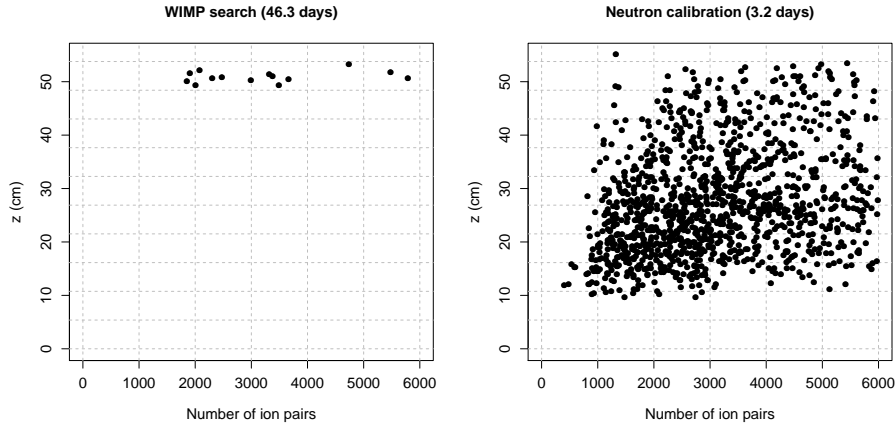


Figure 2: z vs. NIPs distributions of events in the WIMP search and calibration neutron datasets. Events recorded during WIMP-search operation (left panel). No background events appear in the bulk fiducial volume at any energy and this permits the definition of a large background-free signal region below $z = 48.4$ cm, which is shown to be sensitive to neutron recoils, and hence WIMP interactions, by the calibration data (right panel). The grid lines are drawn to match the bins in the efficiency map of Figure 3. The absence of events below $z \sim 10$ cm and the z -dependence of the low-energy cutoff in the neutron calibration data are described in the text.

distributions for events in the WIMP search (46.3 days) and neutron calibration (3.2 days) datasets are shown in Figure 2.

4. Nuclear recoil efficiency

As discussed in Ref. [16], elastic recoils from ^{252}Cf neutrons provide a useful calibration data set. A total of 3.2 live-days of neutron calibration data were taken in 5 dedicated runs interspersed with WIMP-search operation, during which time the ^{252}Cf source was placed on top of the vacuum vessel, inside the shielding. The activity of the source at the time of the exposures varied from 1500 to 1410 neutrons/s with a systematic uncertainty of about 80 neutrons/s [18]. To inhibit gamma ray interactions, the source was contained within a cylindrical lead canister of wall thickness 1.3 cm.

The calculation of the nuclear recoil efficiency proceeded as follows. The parameter space of NIPs vs. z was subdivided into cells as shown in Figure 3, and the number of accepted neutron recoils from the analysis, including all cuts, was calculated for each cell. A detailed GEANT4 simulation of the exposure was run, which included the shielding, the location of the source, the Pb around the source and all detector components. Elastic and inelastic interactions with

nuclei within the fiducial volume had their recoil types, initial energies, and initial interaction locations recorded. The initial recoil energies were converted to NIPs using quenching factors calculated by Hitachi [30]. Thus, the number of GEANT4-generated events for each cell in the NIPs vs. z space could also be calculated. A similar simulation of the DRIFT-IIa detector showed $100 \pm 2\%$ (statistical) $\pm 5\%$ (systematic) efficiency after the Stage 1 cuts and background subtraction for large NIP events [32]. Here we took advantage of that result to normalise (using 3 high efficiency bins: $3000 < \text{NIPs} < 3500$ and $16.1 < z < 32.3$ cm) the GEANT results to events in the neutron calibration data passing the Stage 1 cuts, and a ‘by-eye’ analysis, to remove backgrounds. The ‘by-eye’ analysis also allowed us to calculate the ratio of the number of accepted events after the full set of cuts to the number of accepted events after the Stage 1 cuts. This was found to be 74%. Altogether the counts in each bin for the GEANT4 MC data were reduced by a factor of 2.1 to match the available data. The resulting ratio for each cell (the efficiency map) is shown in Figure 3. Note that by far the most important ratios for limit setting are those at the threshold of detection (~ 1000 NIPs).

The efficiency is zero below $z \sim 10$ cm for two reasons. First, the temporal overlap of the minority peaks reduces the likelihood of a successful reconstruction of z , and events without z -reconstruction are cut from the analysis. Second, the cut on the ratio of charge in the I peak to the charge in the minority peaks has low nuclear recoil acceptance in this regime. The events at low NIPs are cut because of the hardware threshold. The positive slope of the left-hand edge of the neutron events shown in Figure 2 is due to diffusion-broadening of the signal, which causes the peak to fall below threshold. An improved triggering scheme that monitors the integral of the signal, currently under development, could recover these events. The upper limit on z of 48.4 cm was set at $z_{\text{RPR}}^{\text{min}} - 5 \times \Delta z$, where $z_{\text{RPR}}^{\text{min}}$ is the minimum z in the RPR/LEA background distribution shown in the left-hand panel of Figure 2 and Δz is the z -reconstruction precision described above. The advantages of this efficiency map are ease of calculation, freedom from model-dependent parameters (other than GEANT4), complete inclusion of any biases from analysis including difficult-to-model biases from peak fitting, and transparency for others wishing to make use of DRIFT data.

5. WIMP recoil simulation and limits

The calculation of limits proceeded as follows. For an assumed WIMP mass, several thousand fluorine recoils were generated inside a simulated DRIFT-IIa detector using the halo parameters and equations from Ref. [33] ($v_0 = 230$ km/s, $v_E = 244$ km/s and $v_{\text{esc}} = 600$ km/s). The recoils were distributed uniformly in z . As with the GEANT4 simulation, recoil energies were converted to NIPs. A WIMP number matrix was calculated by counting the number of WIMP recoils in each cell of the efficiency map. The detection efficiency was then calculated by multiplying the WIMP number matrix by the efficiency map, summing over all cells and dividing by the total number of recoils. The expected number of detected WIMP recoils was found by multiplying the nominal rate calculated,

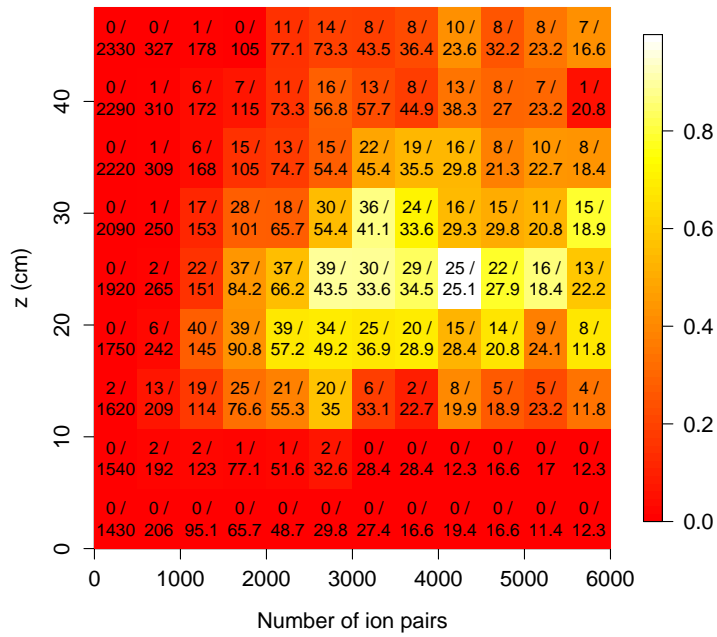


Figure 3: An efficiency map for recoil detection including all analysis cuts. Each cell shows the number of detected recoils over the number expected from the GEANT4 simulation.

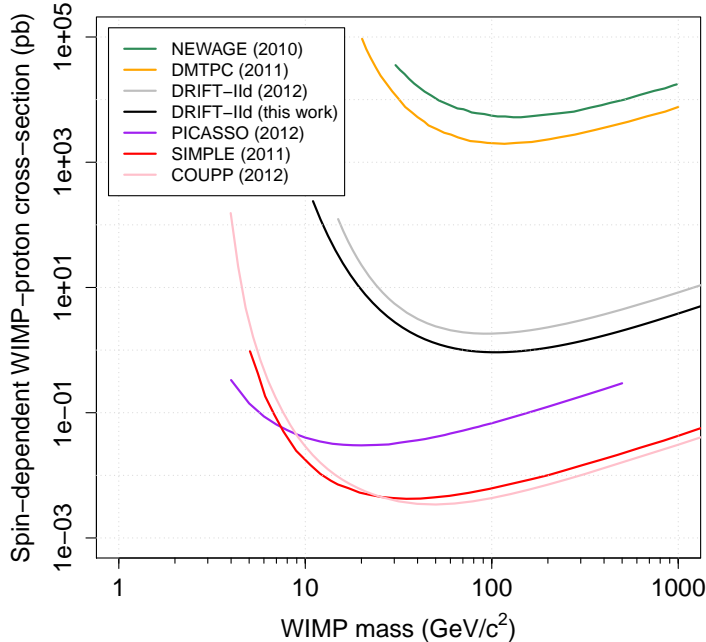


Figure 4: Limits on the spin-dependent WIMP-proton interaction cross section. Limits obtained from these data are shown in black, and the previous limit curve from the DRIFT experiment using a similar live time is shown in grey [23]. All limits from other directional DM detectors (DMTPC [35] and NEWAGE [36]) are also shown. The leading non-directional detector limits are also shown (PICASSO [37], SIMPLE [38] and COUPP [39]).

using the parameters and equations in Ref. [33] ($\rho_D = 0.3 \text{ GeV}/c^2/\text{cm}^3$), by the exposure time (46.3 days) and by the detection efficiency. Including a coherence term [33], this number was used to calculate a WIMP-nucleus exclusion (90% C.L.) cross section. Finally, this was converted to a WIMP-proton spin-dependent cross section using the method of Tovey et al. [34]. This procedure was repeated for a number of WIMP masses, and the resulting data smoothed to produce the exclusion curve shown in Figure 4.

6. Results and discussion

The limit curve shown in Figure 4 improves upon the previous limit from DRIFT by a factor of two [23], and was achieved with comparable live-time (46.3 days vs 47.4 days). The increase in efficiency driving this improvement

is due to the removal of the low-efficiency cuts and the expansion of the signal region. However, because the fixed-amplitude trigger threshold used in this analysis was the same as in the previous work, the effective ionization threshold has increased. This is because $\sim \frac{1}{2}$ of the charge is transferred out of the I peak and into the minority carrier peaks, as discussed above.

Subsequent test runs have demonstrated stable operation of DRIFT-IIId with a threshold that is a factor of two lower than used in this analysis without triggering on electronic noise. This should improve the efficiency by a factor of $\gtrsim 3$. In addition, work is underway to trigger on the pulse integral, rather than on the pulse amplitude. Modifications to the gas flow system have been identified that will permit operation with continuous-flow of the $\text{CS}_2:\text{CF}_4:\text{O}_2$ mixture, rather than as a series of sealed runs. This continuous flow mode of operation will ensure that the oxygen partial pressure, and therefore the relative minority carrier ionisation, remain stable. This is important for maximising the efficiency of the peak-finding algorithm. Finally, improvements to the automated peak-finding analysis are in development, which are expected to improve the efficiency further.

7. Conclusion

Background-free operation of a direction-sensitive WIMP detector with full 3D fiducialisation has been demonstrated for the first time. An analysis of 46.3 live-days of data taken with the directional dark matter detector DRIFT-IIId with fiducialising O_2 additive has produced a limit on the spin-dependent WIMP-proton interaction that is a factor of 2 stronger than previously published by the DRIFT collaboration, with a similar exposure. It is also three orders of magnitude stronger than other directional detectors. The increase in efficiency over our 2012 publication was due to the ability to measure the z -coordinate of events, and therefore reject all known DRIFT-IIId backgrounds. Further increases in efficiency have already been achieved, and other improvements are in development, including reduced trigger threshold. These results expand the reach of directional dark matter detectors.

Acknowledgements

We acknowledge support from the STFC under grant ST/K001337/1, and from the NSF under grant numbers 1103420 and 1103511. JBRB acknowledges support of the Sloan Foundation, and SWS is grateful for STFC grant no. ST/F007337/1. We would also like to thank the owners of Boulby mine, Cleveland Potash Ltd., for their continued support of the underground laboratory.

References

- [1] J. Beringer, J. F. Arguin, R. M. Barnett, K. Copic, O. Dahl, D. E. Groom, C. J. Lin, J. Lys, H. Murayama, C. G. Wohl, W. M. Yao, P. a. Zyla,

- C. Amsler, M. Antonelli, D. M. Asner, H. Baer, H. R. Band, T. Basaglia, C. W. Bauer, Review of particle physics, *Phys. Rev. D* 86 (1) (2012) 010001. doi:10.1103/PhysRevD.86.010001. URL <http://link.aps.org/doi/10.1103/PhysRevD.86.010001>
- [2] J. L. Feng, Dark Matter Candidates from Particle Physics and Methods of Detection, *Annu. Rev. Astron. Astrophys.* (2010) 495–547doi:10.1146/annurev-astro-082708-101659.
- [3] R. Agnese, Z. Ahmed, A. J. Anderson, S. Arrenberg, D. Balakishiyeva, R. Basu Thakur, D. A. Bauer, J. Billard, A. Borgland, D. Brandt, P. L. Brink, T. Bruch, R. Bunker, B. Cabrera, D. O. Caldwell, D. G. Cerdeno, H. Chagani, J. Cooley, B. Cornell, C. H. Crewdson, P. Cushman, M. Daal, F. Dejongh, E. do Couto e Silva, T. Doughty, L. Esteban, S. Fallows, E. Figueroa-Feliciano, J. Filippini, J. Fox, M. Fritts, G. L. Godfrey, S. R. Golwala, J. Hall, R. H. Harris, S. A. Hertel, T. Hofer, D. Holmgren, L. Hsu, M. E. Huber, A. Jastram, O. Kamaev, B. Kara, M. H. Kelsey, A. Kennedy, P. Kim, M. Kiveni, K. Koch, M. Kos, S. W. Leman, B. Loer, E. Lopez Asamar, R. Mahapatra, V. Mandic, C. Martinez, K. A. McCarthy, N. Mirabolfathi, R. A. Moffatt, D. C. Moore, P. Nadeau, R. H. Nelson, K. Page, R. Partridge, M. Pepin, A. Phipps, K. Prasad, M. Pyle, H. Qiu, W. Rau, P. Redl, A. Reisetter, Y. Ricci, T. Saab, B. Sadoulet, J. Sander, K. Schneck, R. W. Schnee, S. Scorza, B. Serfass, B. Shank, D. Speller, K. M. Sundqvist, A. N. Villano, B. Welliver, D. H. Wright, S. Yellin, J. J. Yen, J. Yoo, B. A. Young, J. Zhang, Silicon detector dark matter results from the final exposure of CDMS II, *Phys. Rev. Lett.* 111 (25) (2013) 251301. doi:10.1103/PhysRevLett.111.251301. URL <http://link.aps.org/doi/10.1103/PhysRevLett.111.251301>
- [4] G. Angloher, M. Bauer, I. Bavykina, A. Bento, C. Bucci, C. Ciemniak, G. Deuter, F. Feilitzsch, D. Hauff, P. Huff, C. Isaila, J. Jochum, M. Kiefer, M. Kimmerle, J.-C. Lanfranchi, F. Petricca, S. Pfister, W. Potzel, F. Pröbst, F. Reindl, S. Roth, K. Rottler, C. Sailer, K. Schöffner, J. Schmaler, S. Scholl, W. Seidel, M. V. Sivers, L. Stodolsky, C. Strandhagen, R. Strauß, A. Tanzke, I. Usherov, S. Wawoczny, M. Willers, A. Zöller, Results from 730 kg days of the CRESST-II dark matter search, *Eur. Phys. J. C* 72 (4) (2012) 1971. doi:10.1140/epjc/s10052-012-1971-8. URL <http://www.springerlink.com/index/10.1140/epjc/s10052-012-1971-8>
- [5] R. Bernabei, P. Belli, F. Cappella, R. Cerulli, C. J. Dai, A. D'Angelo, H. L. He, A. Incicchitti, H. H. Kuang, X. H. Ma, F. Montecchia, F. Nozzoli, D. Prospero, X. D. Sheng, R. G. Wang, Z. P. Ye, New results from DAMA/LIBRA, *Eur. Phys. J. C* 67 (2010) 39–49. doi:10.1140/epjc/s10052-010-1303-9. URL <http://www.springerlink.com/index/10.1140/epjc/s10052-010-1303-9>

- [6] C. E. Aalseth, P. S. Barbeau, J. Colaresi, J. I. Collar, J. D. Leon, J. E. Fast, N. E. Fields, T. W. Hossbach, A. Knecht, M. S. Kos, M. G. Marino, H. S. Miley, M. L. Miller, J. L. Orrell, K. M. Yocum, Search for An Annual Modulation in Three Years of CoGeNT Dark Matter Detector Data, arXiv Prepr. arXiv 1401.3295 (2014) 1–8 [arXiv:1401.3295](https://arxiv.org/abs/1401.3295).
URL <http://arxiv.org/abs/1401.3295v1>
- [7] D. S. Akerib, H. M. Araújo, X. Bai, a. J. Bailey, J. Balajthy, S. Bedikian, E. Bernard, A. Bernstein, A. Bolozdynya, A. Bradley, D. Byram, S. B. Cahn, M. C. Carmona-Benitez, C. Chan, J. J. Chapman, a. a. Chiller, C. Chiller, K. Clark, T. Coffey, A. Currie, A. Curioni, S. Dazeley, L. de Viveiros, A. Dobi, J. Dobson, E. M. Dragowsky, E. Druszkiewicz, B. Edwards, C. H. Faham, S. Fiorucci, C. Flores, R. J. Gaitskell, V. M. Gehman, C. Ghag, K. R. Gibson, M. G. D. Gilchriese, C. Hall, M. Hanhardt, S. a. Hertel, M. Horn, D. Q. Huang, M. Ihm, R. G. Jacobsen, L. Kastens, K. Kazkaz, R. Knoche, S. Kyre, R. Lander, N. a. Larsen, C. Lee, D. S. Leonard, K. T. Lesko, A. Lindote, M. I. Lopes, A. Lyashenko, D. C. Malling, R. Mannino, D. N. McKinsey, D.-M. Mei, J. Mock, M. Moongweluwan, J. Morad, M. Morii, A. S. J. Murphy, C. Nehr Korn, H. Nelson, F. Neves, J. a. Nikkel, R. a. Ott, M. Pangilinan, P. D. Parker, E. K. Pease, K. Pech, P. Phelps, L. Reichhart, T. Shutt, C. Silva, W. Skulski, C. J. Sofka, V. N. Solovov, P. Sorensen, T. Stiegler, K. OSullivan, T. J. Sumner, R. Svoboda, M. Sweany, M. Szydagis, D. Taylor, B. Tennyson, D. R. Tiedt, M. Tripathi, S. Uvarov, J. R. Verbus, N. Walsh, R. Webb, J. T. White, D. White, M. S. Witherell, M. Wlasenko, F. L. H. Wolfs, M. Woods, C. Zhang, First Results from the LUX Dark Matter Experiment at the Sanford Underground Research Facility, *Phys. Rev. Lett.* 112 (9) (2014) 091303. doi:10.1103/PhysRevLett.112.091303.
URL <http://link.aps.org/doi/10.1103/PhysRevLett.112.091303>
- [8] E. Aprile, M. Alfonsi, K. Arisaka, F. Arneodo, C. Balan, L. Baudis, B. Bauermeister, A. Behrens, P. Beltrame, K. Bokeloh, E. Brown, G. Bruno, R. Budnik, J. M. R. Cardoso, W.-T. Chen, B. Choi, D. Cline, a. P. Colijn, H. Contreras, J. P. Cussonneau, M. P. Decowski, E. Duchovni, S. Fattori, a. D. Ferella, W. Fulgione, F. Gao, M. Garbini, C. Ghag, K.-L. Giboni, L. W. Goetzke, C. Grignon, E. Gross, W. Hampel, F. Kaether, A. Kish, J. Lamblin, H. Landsman, R. F. Lang, M. Le Calloch, C. Levy, K. E. Lim, Q. Lin, S. Lindemann, M. Lindner, J. a. M. Lopes, K. Lung, T. Marrodán Undagoitia, F. V. Massoli, a. J. Melgarejo Fernandez, Y. Meng, A. Molinario, E. Nativ, K. Ni, U. Oberlack, S. E. a. Orrigo, E. Pantic, R. Persiani, G. Plante, N. Priel, A. Rizzo, S. Rosendahl, J. M. F. dos Santos, G. Sartorelli, J. Schreiner, M. Schumann, L. Scotto Lavina, P. R. Scovell, M. Selvi, P. Shagin, H. Simgen, A. Teymourian, D. Thers, O. Vitells, H. Wang, M. Weber, C. Weinheimer, Dark matter results from 225 live days of XENON100 data, *Phys. Rev. Lett.* 109 (18) (2012) 181301. doi:10.1103/PhysRevLett.109.181301.
URL <http://link.aps.org/doi/10.1103/PhysRevLett.109.181301>

- [9] S. Ahlen, N. Afshordi, J. B. R. Battat, J. Billard, N. Bozorgnia, S. Burgos, T. Caldwell, J. M. Carmona, S. Cebrian, P. Colas, T. Dafni, E. Daw, D. Dujmic, A. Dushkin, W. Fedus, E. Ferrer, D. Finkbeiner, P. H. Fisher, J. Forbes, T. Fusayasu, J. Galan, T. Gamble, C. Ghag, I. Giomataris, M. Gold, H. Gomez, M. E. Gomez, P. Gondolo, A. Green, C. Grignon, O. Guillaudin, C. Hagemann, K. Hattori, S. Henderson, N. Higashi, C. Ida, F. J. Iguaz, A. Inglis, I. G. Irastorza, S. Iwaki, A. Kaboth, S. Kabuki, J. Kadyk, N. Kallivayalil, H. Kubo, S. Kurosawa, V. a. Kudryavtsev, T. Lamy, R. Lanza, T. B. Lawson, A. Lee, E. R. Lee, T. Lin, D. Loomba, J. Lopez, G. Luzon, T. Manobu, J. Martoff, F. Mayet, B. McCLUSKEY, E. Miller, K. Miuchi, J. Monroe, B. Morgan, D. Muna, a. S. J. Murphy, T. Naka, K. Nakamura, M. Nakamura, T. Nakano, G. G. Nicklin, H. Nishimura, K. Niwa, S. M. Paling, J. Parker, A. Petkov, M. Pipe, K. Pushkin, M. Robinson, A. Rodriguez, J. Rodriguez-Quintero, T. Sahin, R. Sanderson, N. Sanghi, D. Santos, O. Sato, T. Sawano, G. Sciolla, H. Sekiya, T. R. Slatyer, D. P. Snowden-Ifft, N. J. C. Spooner, A. Sugiyama, A. Takada, M. Takahashi, A. Takeda, T. Tanimori, K. Taniue, A. Tomas, H. Tomita, K. Tsuchiya, J. Turk, E. Tziaferi, K. Ueno, S. Vahsen, R. Vanderspek, J. Vergados, J. a. Villar, H. Wellenstein, I. Wolfe, R. K. Yamamoto, H. Yegoryan, The Case for a Directional Dark Matter Detector and the Status of Current Experimental Efforts, *Int. J. Mod. Phys. A* 25 (01) (2010) 1. doi:10.1142/S0217751X10048172. URL <http://www.worldscinet.com/ijmpa/25/2501/S0217751X10048172.html>
- [10] C. J. Copi, J. Heo, L. M. Krauss, Directional sensitivity , WIMP detection , and the galactic halo, *Phys. Lett. B* 461 (August) (1999) 43–48.
- [11] B. Morgan, A. Green, N. Spooner, Directional statistics for realistic weakly interacting massive particle direct detection experiments, *Phys. Rev. D* 71 (10) (2005) 103507. doi:10.1103/PhysRevD.71.103507. URL <http://link.aps.org/doi/10.1103/PhysRevD.71.103507>
- [12] A. Green, B. Morgan, Optimizing WIMP directional detectors, *Astropart. Phys.* 27 (2-3) (2007) 142—149. doi:10.1016/j.astropartphys.2006.10.006. URL <http://linkinghub.elsevier.com/retrieve/pii/S0927650506001599>
- [13] D. Nygren, Columnar recombination: a tool for nuclear recoil directional sensitivity in a xenon-based direct detection WIMP search, *J. Phys. Conf. Ser.* 460 (2013) 012006. doi:10.1088/1742-6596/460/1/012006. URL <http://iopscience.iop.org/1742-6596/460/1/012006>
- [14] F. Cappella, R. Bernabei, P. Belli, V. Caracciolo, R. Cerulli, F. a. Danevich, A. D'Angelo, A. Di Marco, A. Incicchitti, D. V. Poda, V. I. Tretyak, On the potentiality of the ZnWO₄ anisotropic detectors to measure the directionality of Dark Matter, *Eur. Phys. J. C* 73 (1) (2013) 2276. doi:

10.1140/epjc/s10052-013-2276-2.

URL <http://link.springer.com/10.1140/epjc/s10052-013-2276-2>

- [15] D. Snowden-Ifft, C. Martoff, J. Burwell, Low pressure negative ion time projection chamber for dark matter search, *Phys. Rev. D* 61 (10) (2000) 101301. doi:10.1103/PhysRevD.61.101301.
URL <http://link.aps.org/doi/10.1103/PhysRevD.61.101301>
- [16] S. Burgos, E. Daw, J. Forbes, C. Ghag, M. Gold, C. Hagemann, V. Kudryavtsev, T. Lawson, D. Loomba, P. Majewski, Measurement of the range component directional signature in a DRIFT-II detector using ^{252}Cf neutrons, *Nucl. Instruments Methods Phys. Res. Sect. A Accel. Spectrometers, Detect. Assoc. Equip.* 600 (2) (2009) 417–423. doi:10.1016/j.nima.2008.11.147.
URL <http://linkinghub.elsevier.com/retrieve/pii/S0168900208017518>
- [17] S. Burgos, E. Daw, J. Forbes, C. Ghag, M. Gold, C. Hagemann, V. Kudryavtsev, T. Lawson, D. Loomba, P. Majewski, First measurement of the headtail directional nuclear recoil signature at energies relevant to WIMP dark matter searches, *Astropart. Phys.* 31 (4) (2009) 261–266. doi:10.1016/j.astropartphys.2009.02.003.
URL <http://linkinghub.elsevier.com/retrieve/pii/S0927650509000310>
- [18] S. Burgos, J. Forbes, C. Ghag, M. Gold, V. Kudryavtsev, T. Lawson, D. Loomba, P. Majewski, D. Muna, A. Murphy, Studies of neutron detection and backgrounds with the DRIFT-IIa dark matter detector, *Astropart. Phys.* 28 (2007) 409–421. doi:10.1016/j.astropartphys.2007.08.007.
URL <http://linkinghub.elsevier.com/retrieve/pii/S0927650507001065>
- [19] J. Battat, J. Brack, E. Daw, Radon in the DRIFT-II directional dark matter TPC: emanation, detection and mitigation, *arXiv Prepr.* arXiv 1407.3938.
URL <http://arxiv.org/abs/1407.3938>
- [20] J. Brack, E. Daw, A. Dorofeev, a. C. Ezeribe, J. R. Fox, J. L. Gauvreau, M. Gold, L. J. Harmon, J. Harton, R. Lafler, J. M. Landers, R. Lauer, E. R. Lee, D. Loomba, J. a. J. Matthews, E. H. Miller, A. Monte, a. S. Murphy, S. M. Paling, N. Phan, M. Pipe, M. Robinson, S. Sadler, A. Scarff, D. P. Snowden-Ifft, N. J. C. Spooner, S. Telfer, D. Walker, L. Yuriev, Long-term study of backgrounds in the DRIFT-II directional dark matter experiment, *J. Instrum.* 9. arXiv:1307.5525.
URL <http://arxiv.org/abs/1307.5525v3>
- [21] J. Brack, E. Daw, A. Dorofeev, A. Ezeribe, J.-L. Gauvreau, M. Gold, J. Harton, R. Lafler, R. Lauer, E. R. Lee, D. Loomba, J. Matthews, E. H. Miller, A. Monte, A. Murphy, S. Paling, N. Phan, S. Sadler, A. Scarff,

- D. Snowden-Ifft, N. Spooner, S. Telfer, D. Walker, M. Williams, L. Yuriev, Background Assay and Rejection in DRIFT, *Phys. Procedia* 00 (2014) 1–7. [arXiv:1404.2253](https://arxiv.org/abs/1404.2253).
URL <http://arxiv.org/abs/1404.2253v1>
- [22] D. Snowden-Ifft, Discovery of multiple, ionization-created anions in gas mixtures containing CS₂ and O₂, *Rev. Sci. Instrum.* 85 (1) (2014) 013303. URL <http://arxiv.org/abs/1308.0354>
- [23] E. Daw, J. R. Fox, J. Gauvreau, C. Ghag, Spin-dependent limits from the DRIFT-II_d directional dark matter detector, *Astropart. Phys.* 35 (7) (2012) 397–401. URL <http://arxiv.org/abs/1010.3027><http://www.sciencedirect.com/science/article/pii/S0927650511002027>
- [24] S. M. Paling, A. S. J. Murphy, The Boulby Mine Underground Science Facility: the search for dark matter, and beyond, *Nucl. Phys. News* 22 (1). URL <http://www.tandfonline.com/doi/abs/10.1080/10619127.2011.629920#.UeU4zz7TUyU>
- [25] G. Alner, H. Araujo, A. Bewick, S. Burgos, M. Carson, J. Davies, E. Daw, J. Dawson, J. Forbes, T. Gamble, The DRIFT-II dark matter detector: design and commissioning, *Nucl. Instruments Methods Phys. Res. Sect. A Accel. Spectrometers, Detect. Assoc. Equip.* 555 (1-2) (2005) 173–183. doi:10.1016/j.nima.2005.09.011. URL <http://linkinghub.elsevier.com/retrieve/pii/S0168900205018139>
- [26] K. Pushkin, D. Snowden-Ifft, Measurements of W-value, mobility and gas gain in electronegative gaseous CS₂ and CS₂ gas mixtures, *Nucl. Instruments Methods Phys. Res. Sect. A Accel. Spectrometers, Detect. Assoc. Equip.* 606 (3) (2009) 569–577. doi:10.1016/j.nima.2009.04.045. URL <http://linkinghub.elsevier.com/retrieve/pii/S0168900209008985>
- [27] W. Haerberli, P. Huber, E. Baldinger, Work per ion pair in gas mixtures for alpha particles, *Helv. Phys. Acta* 26.
- [28] H. J. Moe, T. E. Bortner, G. S. Hurst, Ionization of Acetylene Mixtures and Other Mixtures by Pu²³⁹ Alpha Particles, *J. Phys. Chem.* 61 (4).
- [29] M. Kimura, K. Kowari, M. Inokuti, I. Bronić, Theoretical Study of W Values in Hydrocarbon Gases, *Radiat. Res.* 125 (3) (1991) 237–242. URL <http://www.rrjournal.org/doi/abs/10.2307/3578104>
- [30] A. Hitachi, Bragg-like curve for dark matter searches: binary gases, *Radiat. Phys. Chem.* 77 (10–12) (2008) 1311–1317. doi:10.1016/j.radphyschem.2008.05.044. URL <http://linkinghub.elsevier.com/retrieve/pii/S0969806X08001436>

- [31] D. Snowden-Ifft, T. Ohnuki, E. Rykoff, C. Martoff, Neutron recoils in the DRIFT detector, *Nucl. Instruments Methods Phys. Res. Sect. A Accel. Spectrometers, Detect. Assoc. Equip.* 498 (1-3) (2003) 155—164. doi:10.1016/S0168-9002(02)02120-4.
URL <http://linkinghub.elsevier.com/retrieve/pii/S0168900202021204>
- [32] S. Agostinelli, J. Allison, K. Amako, J. Apostolakis, H. Araujo, P. Arce, M. Asai, D. Axen, S. Banerjee, G. Barrand, F. Behner, L. Bellagamba, J. Boudreau, L. Broglia, A. Brunengo, H. Burkhardt, S. Chauvie, J. Chuma, R. Chytrcek, G. Cooperman, G. Cosmo, P. Degtyarenko, A. Dell’Acqua, G. Depaola, D. Dietrich, R. Enami, A. Feliciello, C. Ferguson, H. Fesefeldt, G. Folger, F. Foppiano, A. Forti, S. Garelli, S. Giani, R. Giannitrapani, D. Gibin, J. Gómez Cadenas, I. González, G. Gracia Abril, G. Greeniaus, W. Greiner, V. Grichine, A. Grossheim, S. Guatelli, P. Gumplinger, R. Hamatsu, K. Hashimoto, H. Hasui, A. Heikkinen, A. Howard, V. Ivanchenko, A. Johnson, F. Jones, J. Kallenbach, N. Kanaya, M. Kawabata, Y. Kawabata, M. Kawaguti, S. Kelner, P. Kent, A. Kimura, T. Kodama, R. Kokoulin, M. Kossov, H. Kurashige, E. Lamanna, T. Lampén, V. Lara, V. Lefebure, F. Lei, M. Liendl, W. Lockman, F. Longo, S. Magni, M. Maire, E. Medernach, K. Minamimoto, P. Mora de Freitas, Y. Morita, K. Murakami, M. Nagamatu, R. Nartallo, P. Nieminen, T. Nishimura, K. Ohtsubo, M. Okamura, S. O’Neale, Y. Oohata, K. Paech, J. Perl, A. Pfeiffer, M. Pia, F. Ranjard, A. Rybin, S. Sadilov, E. Di Salvo, G. Santin, T. Sasaki, N. Savvas, Y. Sawada, S. Scherer, S. Sei, V. Sirotenko, D. Smith, N. Starkov, H. Stoecker, J. Sulkimo, M. Takahata, S. Tanaka, E. Tcherniaev, E. Safai Tehrani, M. Tropeano, P. Truscott, H. Uno, L. Urban, P. Urban, M. Verderi, A. Walkden, W. Wander, H. Weber, J. Wellisch, T. Wenaus, D. Williams, D. Wright, T. Yamada, H. Yoshida, D. Zschesche, Geant4a simulation toolkit, *Nucl. Instruments Methods Phys. Res. Sect. A Accel. Spectrometers, Detect. Assoc. Equip.* 506 (3) (2003) 250–303. doi:10.1016/S0168-9002(03)01368-8.
URL <http://linkinghub.elsevier.com/retrieve/pii/S0168900203013688>
- [33] J. D. Lewin, P. Smith, Review of mathematics, numerical factors, and corrections for dark matter experiments based on elastic nuclear recoil, *Astropart. Phys.* 6 (96) (1996) 87—112.
URL <http://www.sciencedirect.com/science/article/pii/S0927650596000473>
- [34] D. R. Tovey, R. J. Gaitskell, P. Gondolo, Y. Ramachers, L. Roszkowski, A new model-independent method for extracting spin-dependent cross section limits from dark matter searches, *Phys. Lett. B* 488 (2000) 17—26.
URL <http://www.sciencedirect.com/science/article/pii/S0370269300008467>

- [35] S. Ahlen, J. Battat, T. Caldwell, C. Deaconu, D. Dujmic, W. Fedus, P. Fisher, F. Golub, S. Henderson, A. Inglis, A. Kaboth, G. Kohse, R. Lanza, A. Lee, J. Lopez, J. Monroe, T. Sahin, G. Sciolla, N. Skvorodnev, H. Tomita, H. Wellenstein, I. Wolfe, R. Yamamoto, H. Yegoryan, First dark matter search results from a surface run of the 10-L DMTPC directional dark matter detector, *Phys. Lett. B* 695 (1-4) (2011) 124–129. doi:10.1016/j.physletb.2010.11.041.
URL <http://linkinghub.elsevier.com/retrieve/pii/S037026931001316X>
- [36] K. Miuchi, H. Nishimura, K. Hattori, N. Higashi, C. Ida, S. Iwaki, S. Kabuki, H. Kubo, S. Kurosawa, K. Nakamura, J. Parker, T. Sawano, M. Takahashi, T. Tanimori, K. Taniue, K. Ueno, H. Sekiya, A. Takeda, K. Tsuchiya, A. Takada, First underground results with NEWAGE-0.3a direction-sensitive dark matter detector, *Phys. Lett. B* 686 (1) (2010) 11–17. doi:10.1016/j.physletb.2010.02.028.
URL <http://linkinghub.elsevier.com/retrieve/pii/S0370269310002029>
- [37] S. Archambault, E. Behnke, P. Bhattacharjee, S. Bhattacharya, X. Dai, M. Das, a. Davour, F. Debris, N. Dhungana, J. Farine, S. Gagnebin, G. Giroux, E. Grace, C. Jackson, a. Kamaha, C. Krauss, S. Kumaratunga, M. Lafrenière, M. Laurin, I. Lawson, L. Lessard, I. Levine, C. Levy, R. MacDonald, D. Marlisov, J.-P. Martin, P. Mitra, a.J. Noble, M.-C. Piro, R. Podviyanuk, S. Pospisil, S. Saha, O. Scallon, S. Seth, N. Starinski, I. Stekl, U. Wichoski, T. Xie, V. Zacek, Constraints on low-mass WIMP interactions on ^{19}F from PICASSO, *Phys. Lett. B* 711 (2) (2012) 153–161. doi:10.1016/j.physletb.2012.03.078.
URL <http://linkinghub.elsevier.com/retrieve/pii/S0370269312003760>
- [38] M. Felizardo, T. A. Girard, T. Morlat, A. C. Fernandes, Final analysis and results of the phase II SIMPLE dark matter search, *Phys. Rev. Lett.* 108 (2012) 4–7. arXiv:arXiv:1106.3014v3.
URL <http://prl.aps.org/abstract/PRL/v108/i20/e201302>
- [39] E. Behnke, J. Behnke, S. J. Brice, D. Broemmelsiek, First dark matter search results from a 4-kg CF $_3$ I bubble chamber operated in a deep underground site, *Phys. Rev. D* 86 (5) (2012) 052001. arXiv:arXiv:1204.3094v2.
URL <http://prd.aps.org/abstract/PRD/v86/i5/e052001>